Journal of Materials Chemistry A

Accepted Manuscript

ROYAL SOCIETY OF CHEMISTRY

www.rsc.org/materialsA

Journal Name

ARTICLE

Fully-solution-processed organic solar cells with a highly efficient paper-based light trapping element

Received 00th January 20xx,
Accepted 00th January 20xx

DOI: 10.1039/x0xx00000x

www.rsc.org/

Zheng Tang,[a]* Anders Elfwing,[a] Armantas Melianas,[a] Jonas Bergqvist,[a] Qinye Bao,[b] Olle Inganäs[a]*

We demonstrate the use of low cost paper as an efficient light-trapping element for thin film photovoltaics. We verify its use in fully-solution processed organic photovoltaic devices with the highest power conversion efficiency and the lowest internal electrical losses reported so far, the architecture of which – unlike most of the studied geometries to date – is suitable for upscaling, i.e. commercialization. The use of the paper-reflector enhances the external quantum efficiency (EQE) of the organic photovoltaic device by a factor of ≈1.5-2.5 over the solar spectrum, which rivals the light harvesting efficiency of a highly-reflective but also considerably more expensive silver mirror back-reflector. Moreover, by detailed theoretical and experimental analysis, we show that further improvements in the photovoltaic performance of organic solar cells employing PEDOT:PSS as both electrodes rely on the future development of high-conductivity and high-transmittance PEDOT:PSS. This is due optical losses in the PEDOT:PSS electrodes.

Introduction

Organic bulk-heterojunction (BHJ) solar cells, allowing for low cost roll-to-roll production on flexible substrates, are a promising alternative to conventional solar cells. State-of-the-art organic solar cells with power conversion efficiency (PCE) over 10% have been reported, both in single-junction[1] and multi-junction configurations.[2,3] However, most of the reported high efficiency organic solar cells are based on device geometries that are not low cost: the use of (1) a thermally evaporated light-reflecting electrode and (2) a sputtered transparent ITO electrode; both lead to high production and material costs, making such device geometries undesirable for commercial applications.[4,5]

Successful commercialization of organic solar cells requires scalable and inexpensive materials in alternative geometries, which are compatible with roll-to-roll processing. One such promising fully-solution-processable device geometry is the PEDOT-PEDOT solar cell, where the transparent and conductive doped polymer Poly(3,4-ethylenedioxythiophene):Polystyrene sulfonate (PEDOT:PSS) is used as both the anode and the cathode. Although this device geometry requires a modification of at least one of the PEDOT:PSS electrodes to facilitate electron injection, successful modification has already been demonstrated with a number of different interface materials.[6–8] In a recent report, PEDOT-PEDOT devices were constructed by film transfer lamination.[9] A record power conversion efficiency (PCE) of 2.4% was achieved, however still significantly lower than that of a standard solar cell. The lower photovoltaic performance of PEDOT-PEDOT devices as compared to the standard geometry is in part due to the absence of a back-reflecting electrode, which leads to a substantial loss of photons to transmission. This semi-transparency is desired for window integrated photovoltaic applications, although at a cost of reduced photovoltaic performance.[10] However, transmitted photons could be reutilized (back-reflected) by the use of a separately attached light-reflector.[11-13] In fact, such an approach is even desirable as the semi-transparent PEDOT-PEDOT solar cells are optically superior to conventional organic solar cells: due to the lower refractive indexes of the substrate and the PEDOT:PSS electrodes as compared to those of the active layer. Concomitantly, the PEDOT-PEDOT device structure in principle allows for photon trapping in the cell by total-internal-reflection, if a proper light-trapping element, such as, a grating structure[12] or a dielectric light scatterer is employed.[13]

A low-cost light-trapping solution is paper – an easily accessible light-scattering element, which has been demonstrated to work as an anti-reflecting layer[14] or substrate[15,16] for light to enter organic solar cells. However, for efficient light-trapping by total-internal reflection in semi-transparent solar cells, optical conformal contact between the rough surface of the paper and the cell substrate is necessary. So far, due to difficulties in achieving conformal optical contact at the paper/cell interface, there have been no reports of efficient paper based reflectors.

[a] Biomolecular and Organic Electronics, IFM, and Center of Organic Electronics, Linköping University, SE-581 83 Linköping, Sweden. *E-mail: zheng.tang@liu.se, olle.inganas@ifm.liu.se
[b] Surface physics and chemistry, IFM, Linköping University, SE-581 83 Linköping, Sweden.

Electronic Supplementary Information (ESI) available: [details of any supplementary information available should be included here]. See DOI: 10.1039/x0xx00000x

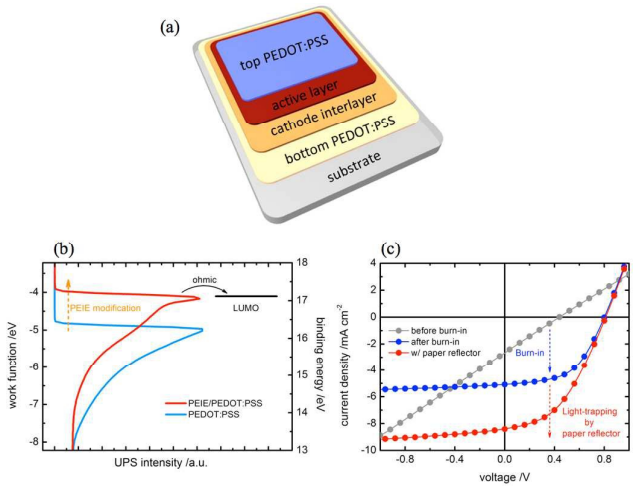

Figure 1. a) Schematic device architecture of a solar cell with PEDOT:PSS as both electrodes. b) Ultra-violet photoemission spectroscopy (UPS) spectra of PEDOT:PSS before and after the PEIE surface modification. The formation of an ohmic contact between the modified PEDOT:PSS electrode and the active layer is indicated schematically. c) Current voltage (JV) characteristic curves of a representative PEDOT-PEDOT solar cell. Device performance parameters are listed in Table S1 (Electronic Supplementary Information).

Here, we report a solution, which allows low cost paper to be used as an efficient light-trapping element. Conformal optical contact at the paper/cell interface is achieved by the use of the inexpensive poly(dimethylsiloxane) (PDMS). We first show that electrical shorts, a common problem in fully-solution-processed devices, can be eliminated by using a PSS cross-linker and by passing a high reverse current through the solar cell. Following the elimination of electrical shorts and proper modification of the bottom PEDOT:PSS electrode, the active layer performs just as well as in standard device geometry, i.e. at an internal quantum efficiency (IQE) of 85%:[17] This is the lowest internal electrical loss reported for fully-solution-processed solar cells.[18-21] We then demonstrate that a paper based reflector enhances the external quantum efficiency (EQE) of the PEDOT-PEDOT solar cell by a factor of ≈1.5-2.5 over the solar spectrum and thus significantly rivals the light harvesting efficiency of a silver mirror back-reflector. A new record PCE for fully-solution-processed solar cell is now set to 4% with the help of the paper reflector. By detailed analyzing theoretical predictions and experimental data, we identify the trade-off between electrical and optical losses, and their effects on the photovoltaic performance of PEDOT-PEDOT solar cells.

Fully solution processed semi-transparent solar cells

Device construction and optimization

A schematic picture of the device architecture of a solar cell with PEDOT:PSS being both the cathode and the anode is given in **Figure 1**a. Such a solar cell is referred to as the PEDOT-PEDOT solar cell. In this work, both the bottom and the top PEDOT:PSS electrodes are deposited from aqueous PEDOT:PSS PH1000 solution mixed with 5% dimethyl sulfoxide.[22] The conductivity of PEDOT:PSS is ≈500 S cm^{-1}. The BHJ active layer is based on a mixture of poly[2,3-bis-(3-octyloxyphenyl)quinoxaline-5,8-diyl-alt-thiophene-2,5-diyl] (TQ1)[23] and [6,6]-phenyl-C71-butyric acid methyl ester ($PC_{71}BM$) with a stoichiometry of 2:5. Material structures are given in Figure S1 of the Electronic Supplementary Information (ESI).

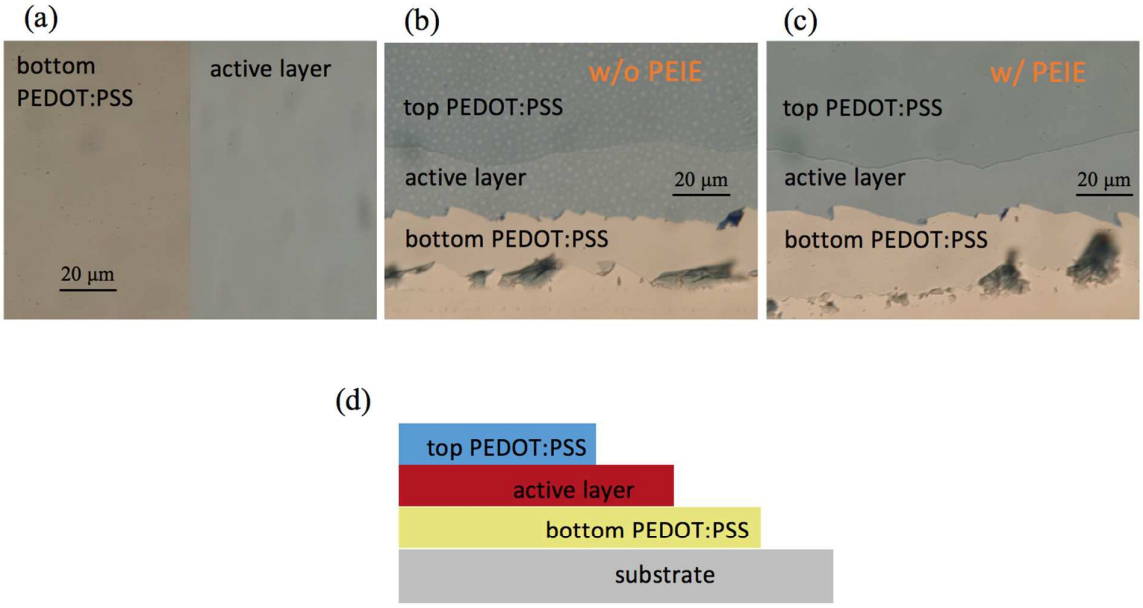

Figure 2. Optical microscopy images of a PEDOT-PEDOT solar cell with and without the PEIE interlayer. a) Before deposition of the top PEDOT:PSS electrode we observe no pin-holes neither in the bottom PEDOT:PSS layer nor in the active layer. b) Deposition of the top PEDOT:PSS electrode induces pin-holes in the active layer, which severely short-circuits the photovoltaic device. c) Upon the use of the PEIE interlayer on top of the bottom PEDOT electrode, pin-holes are barely visible, suggesting that the density and/or size of the pin-holes is significantly reduced. Concomitantly, the PEDOT-PEDOT solar cell with the PEIE interlayer performs significantly better, i.e. we observe no indication of electrical-shorts after burn-in. d) a schematic picture of the sample structure.

A conjugated polymer interlayer polyethylenimine ethoxylated (PEIE)[7] was used to reduce the work function of the bottom PEDOT:PSS electrode to 4.3 eV (Figure 1b), which facilitates electron injection from the modified PEDOT:PSS to the BHJ active layer of the solar cell. The unmodified PEDOT:PSS has a work function of ~5 eV, which is sufficiently high for efficient hole injection, and was therefore left unmodified.

All layers of the PEDOT-PEDOT solar cell are deposited from solution, and they are highly prone to electrical shorts. In fact, we find that all devices prepared without the PEIE interlayer modification are completely electrically shorted. We propose that the reason for electrical shorts is the swelling of the bottom PEDOT:PSS electrode upon deposition of the top PEDOT:PSS electrode. As the thin active layer is permeable to water from the top PEDOT:PSS solution, this causes significant volume changes of the bottom PEDOT:PSS electrode.[24] This in turn leads to micro cracks and pin-hole formation in the active layer, i.e. electrical shorts, as shown in **Figure 2**. We find that the use of the PEIE interlayer alleviates the problem and enables fabrication of working PEDOT-PEDOT solar cells.

Although the use of the PEIE interlayer enables working photovoltaic devices, their performance is still severely limited by the remaining electrical shorts, as indicated by the high shunt current marked 'before burn-in' in Figure 1c. Thicker active layers would often alleviate the problem, however the low charge carrier mobility in organic solar cells then leads to significant carrier recombination losses and thus a poor photovoltaic performance. To solve the problem we have: (1) employed silquest A187, a silane based PSS cross-linker, into the PEDOT:PSS solution for the bottom PEDOT:PSS deposition. PSS cross-linking allows the PEDOT:PSS layer to 'stick' considerably better to the substrate,[25] which in turn reduces the amount of volume change when the bottom PEDOT:PSS layer is exposed to water, coming from the top PEDOT:PSS solution (Figure S2, ESI); (2) applied a strong reverse bias (-20 V for a 5 mm^2 device), which we further refer to as burn-in. Due to the high local reverse current and thus a high temperature at the electrically shorted spots: electrical shorts are burned away. We now confirm this hypothesis experimentally.

Figure 3 shows the map of photocurrent generation under short-circuit conditions, before and after the burn-in, as measured by the light-beam induced current (LBIC) technique.[26] Prior to burn-in, the photoactive area generates only a small amount of photocurrent,

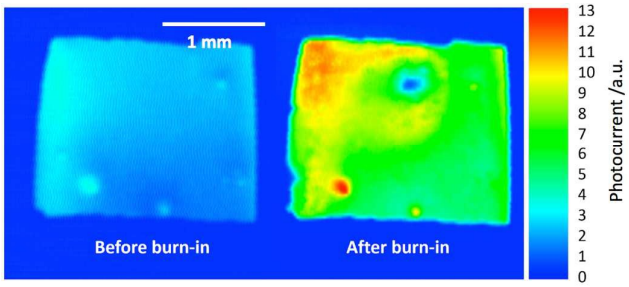

Figure 3. Photocurrent images of a PEDOT-PEDOT solar cell at short-circuit conditions before and after the burn-in.

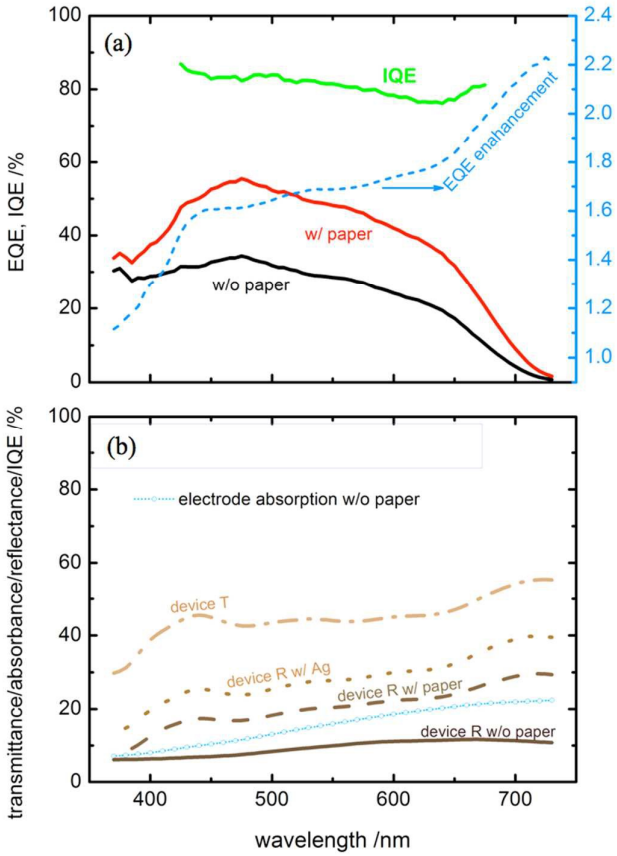

Figure 4. a) EQE, EQE enhancement and IQE of a representative PEDOT-PEDOT solar cell with and without a paper reflector. b) Device transmittance, reflectance, electrode absorbance.

e.g. compare the color scale to the photocurrent image before burn-in. Following burn-in the overall photocurrent extraction from the solar cell is significantly improved, however some spots that do not generate photocurrent remain, e.g. see the small blue region surrounded by an otherwise uniformly green area. We propose that these spots were originally the most electrically shorted and were carbonized due to the high local temperature during the burn-in. It should be noted that due to the limited resolution of the photocurrent imaging technique, the burn-in effect is observed only when the shorted area is large enough. Electrically shorted spots smaller than the resolution of the imaging technique, although not evidently visible, might be present before burn-in i.e. distributed over some area that generates low photocurrent. Nevertheless, despite the slightly reduced electrically active area of the photovoltaic cell after the burn-in, the overall photovoltaic performance is improved dramatically (Figure 1c).

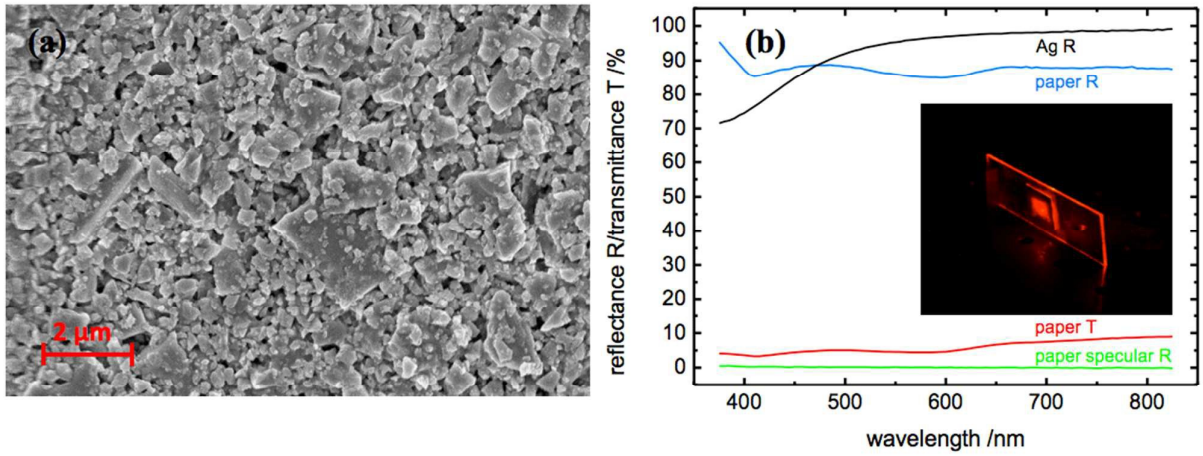

Figure 5. a) Scanning electron microscope (SEM) image of the surface of the paper reflector. b) Reflectance, specular reflectance and transmittance of the paper reflector, and reflectance of a silver planar mirror used as a reference. Inset: a photograph showing the effect of light-trapping by total-internal-reflection in glass, as facilitated by the PDMS coated paper reflector.

Device characterization and effect of the paper based light trapping element

In fact, the active layer performs just as well as in standard device geometry, as indicated by similarly high IQE ≈80-85% over the absorbing wavelength range (**Figure 4a**) and a comparable open-circuit voltage (Voc) ≈0.8V.[17,27] Thus, no additional electrical losses are induced at the modified bottom PEDOT:PSS and active layer interface i.e. contacts are ohmic as in standard device geometry. Therefore a well-performing active layer is achieved. However, as this is a semi-transparent solar cell, a large fraction, ≈45%, of photons is still transmitted (Figure 4b), thereby limiting the power output of such a device. We now add a paper based back-reflector to reutilize the transmitted photons by efficient light-trapping in the active layer.

The paper reflector is based on commercially available paper from StoraEnso by the name of Lumipress Silk. Its good mechanical properties allow to coat PDMS directly on top of it (Figure S3, SI). The paper surface has a coating layer that mainly consists of calcium carbonate and latex. Calcium carbonate is in form of nano-particles with diameters of tens of nanometers to a few micrometers, as indicated by the scanning electron microscope (SEM) images (**Figure 5a**). Therefore, the paper surface is highly diffuse-reflective, i.e. incident light is reflected at many angles. Although the absolute reflectance of such a paper reflector is slightly lower as compared to that of a silver planar mirror (Figure 5b), no specular reflectance is found for the paper, i.e. no light is reflected at the angle of incoming light as is the case for a silver planar mirror. This feature of the paper reflector in principle allows for efficient light-trapping by total-internal-reflection.

However, for total-internal-reflection conformal optical contact between the cell substrate and the paper reflector is also necessary. We find that after curing of PDMS on top of the paper surface, conformal optical contact is indeed formed, and facilitates the desired return of light back into the cell regardless of the angle of incidence. The formation of conformal optical contact between the PDMS coated paper and the glass substrate is confirmed by the illustrative experiment in the inset of Figure 5b. A red laser is illuminating the paper reflector, placed conformally behind the glass slide. A large percentage of light is scattered back with angles larger than the critical angle, therefore scattered light cannot escape the glass. Light mostly escapes at the edges of the glass slide, which are distant from the paper reflector. This demonstrates that PDMS coated paper indeed facilitates efficient light-trapping. Most importantly, this is not just a proof-of-concept in a lab-scale device – the PDMS layer is robust enough to be also used for the development of large-scale photovoltaic modules.

The effect of the integrated paper reflector on the EQE spectra of the PEDOT-PEDOT solar cell is shown in Figure 4a. Light-trapping enhances absorption and concomitantly the EQE of the photovoltaic device by a factor of ~1.7. At wavelengths larger than 670 nm, we observe an EQE enhancement larger than a factor of two: an indication that more photons are absorbed in the active layer during the second and higher order passes of light as compared to the amount of photons absorbed during the first pass. Efficient light-trapping and photon-reutilization is further supported by device reflectance measurements. As shown in Figure 4b, reflectance losses in the PEDOT-PEDOT device with an integrated paper reflector are much smaller as compared to those in a device with an integrated silver mirror. However, the fill factor (FF) of the PEDOT-PEDOT device with the integrated paper reflector is reduced, the origin of which is the high series resistance of PEDOT electrodes. This problem is alleviated by increasing the thickness, i.e. decreasing the resistance, of the bottom PEDOT electrode, as described in a later section.

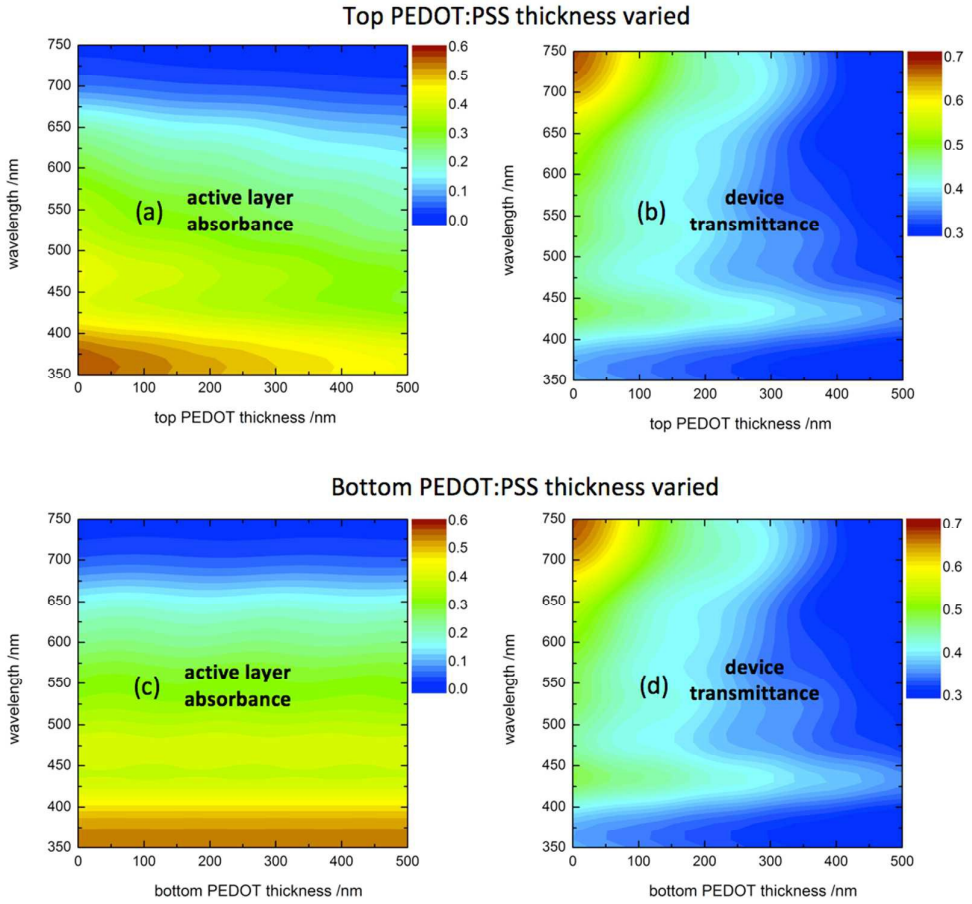

Figure 6. a) Active layer absorption and b) device transmittance simulated with the transfer matrix model for a PEDOT-PEDOT solar cell with a 120 nm bottom PEDOT:PSS electrode, 80 nm active layer, and different thicknesses of the top PEDOT:PSS. c) Active layer absorption and d) device transmittance for a PEDOT-PEDOT solar cell with a 120 nm top PEDOT:PSS electrode, 80 nm active layer, and different thicknesses of the bottom PEDOT:PSS electrode.

Optical and electric losses in PEDOT-PEDOT solar cells

Nevertheless, despite favorable optical performance and significant photocurrent enhancement we find that the large series resistance of PEDOT:PSS electrodes significantly limits the FF of the operating device. This in turn limits the effect of the integrated paper reflector, as can be inspected from the JV curves in Figure 1c and understood by the following observation: Although the short-circuit photocurrent density, which is less affected by the series resistance, is enhanced by a factor as large as ~1.7, the PCE of the PEDOT-PEDOT solar cell upon using the paper reflector is enhanced only by a factor of ~1.4. We further address this issue by reducing the series resistance.

Series resistance can be reduced by the use of thicker PEDOT:PSS electrodes. However, as PEDOT:PSS absorption overlaps with that of the active layer (Figure S4, ESI), increasing the top PEDOT:PSS electrode thickness will in turn reduce absorption in the active layer. To investigate the influence of varying thickness of both PEDOT:PSS electrodes, we have performed optical simulations by the transfer matrix model (**Figure 6**).[28]

Figure 6 indicates that increasing the thickness of the top PEDOT:PSS electrode is not an option. The strong absorption by the top PEDOT:PSS electrode in the range 500-700 nm, significantly reduces the absorption in the active layer (Figure 6a). On the other hand, increasing the thickness of the bottom PEDOT:PSS electrode, only reduces device transmittance (Figure 6d), and, most importantly, barely affects the absorption in the active layer (Figure 6c). This is due to the fact that optical interference effects are weak in PEDOT-PEDOT solar cells on glass or plastic substrates. Optical simulations therefore suggest that to reduce the series resistance it is the bottom PEDOT:PSS electrode that should be made thicker.

However, note that increasing the bottom PEDOT:PSS thickness also leads to a reduction in the transmission of photons, which could have been otherwise reutilized by the integrated paper reflector. The trade-off between increasing active layer absorption by the use of the paper reflector and reducing the series resistance is further investigated experimentally.

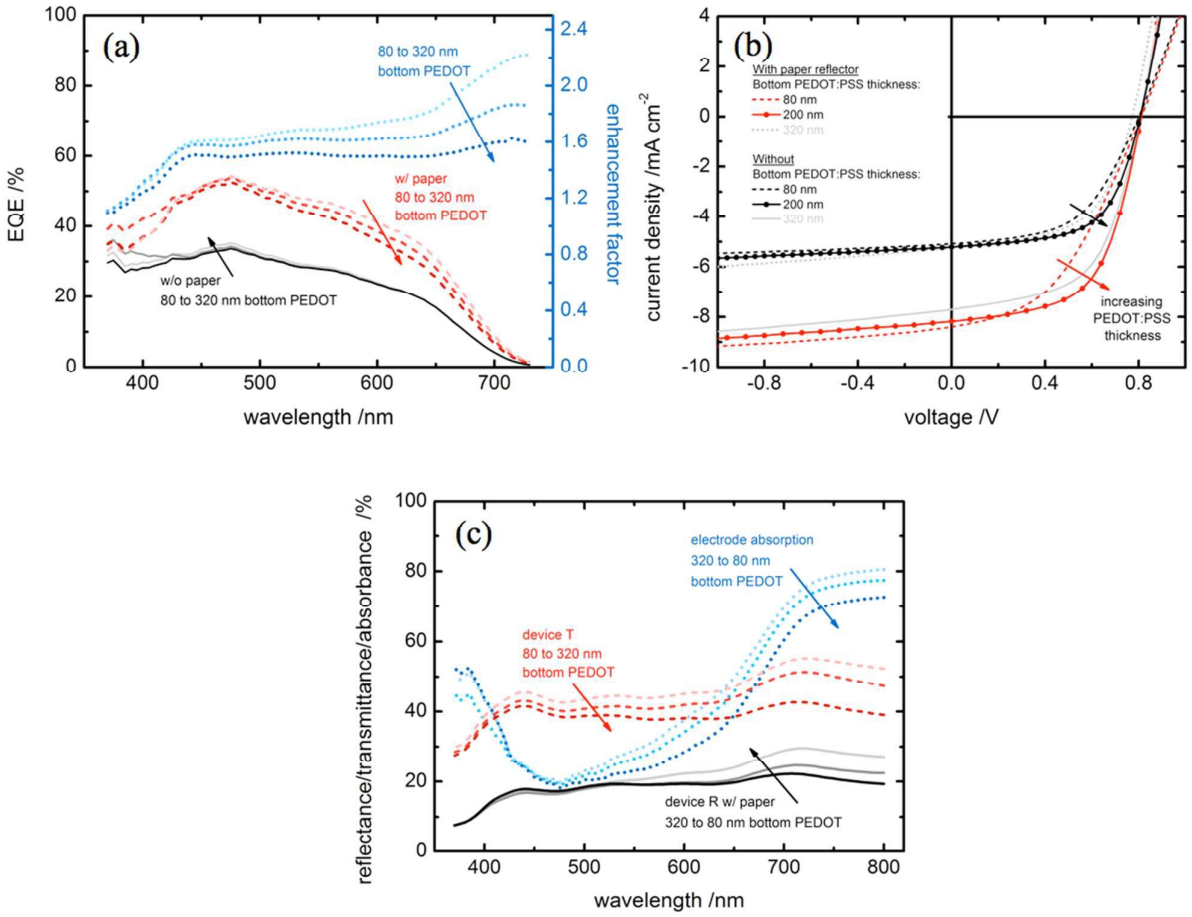

Figure 7. a) EQE of PEDOT-PEDOT solar cells at indicated bottom PEDOT:PSS electrode thicknesses with and without the paper reflector. b) JV characteristic curves of PEDOT-PEDOT solar cells with 80, 200, 320 nm bottom PEDOT:PSS electrodes with and without the paper reflector. c) Device transmittance and electrode absorption of PEDOT-PEDOT solar cells with different thicknesses of the bottom PEDOT:PSS electrode.

Figure 7a shows the effect of various bottom PEDOT:PSS electrode thicknesses on the EQE spectra. Experimental results confirm the before-mentioned optical model predictions. For devices without the paper reflector, increasing the bottom PEDOT:PSS thickness does not reduce the amount of absorbed photons in the active layer, which is reflected by the EQE being insensitive to the bottom PEDOT:PSS thickness. This is further confirmed by the same short-circuit photocurrent density, as can be inspected from the JV curves in Figure 7b. Most importantly, the series resistance is significantly reduced, thereby improving the FF and the overall photovoltaic performance of the device. A PEDOT-PEDOT solar with a PCE of 2.54% is achieved.

Nevertheless the predicted loss of transmitted photons due to PEDOT:PSS absorption remains, as can be inspected from Figure 7c. We can quantify such optical losses due to electrode absorption via:[29]

$$A_{loss}\,(\lambda) = 1 - R(\lambda) - EQE(\lambda)\,/\,IQE(\lambda)$$

where R is device reflectance, and λ is wavelength. Figure 7c shows that electrode absorption losses in solar cells with a thicker bottom PEDOT:PSS electrode are higher in the wavelength range between 500 nm and 750 nm, i.e. precisely where PEDOT:PSS absorbs, see Figure S4, ESI. Thereby confirming that the transmitted photons are indeed lost due to PEDOT:PSS absorption. This in turn reduces the amount of photons reutilized by light-trapping, i.e. EQE enhancement factor is reduced (Figure 7a), especially in the wavelength region where PEDOT:PSS absorbs, thereby directly limiting the benefits of efficient light-trapping.

Despite the additional optical losses (PEDOT:PSS absorption), the photovoltaic performance of the PEDOT-PEDOT solar with the paper reflector is dramatically improved as the thickness of the bottom PEDOT:PSS electrode is increased to 200 nm. This is due to the considerably lower series resistance of the thicker bottom PEDOT:PSS electrode (Figure 7b), resulting in a record PCE of close to 4% for the PEDOT-PEDOT solar cell with an integrated paper reflector.

Further thickness increase of the bottom PEDOT:PSS electrode does not lead to improved device performance, which is due to the following: although, the series resistance is further reduced, we observe increasingly high shunt currents at increasing PEDOT:PSS thickness (Figure 7b), thereby limiting the FF. We propose that the origin of shunt currents is associated to the before-mentioned swelling of the bottom PEDOT:PSS electrode, upon deposition of the top PEDOT:PSS electrode. This effect is more pronounced in thicker PEDOT:PSS electrode films as they swell more and thus deform the active layer, and leads to pin-holes in the active layer.

Conclusions

We have successfully combined a low-cost light trapping scheme with fully-solution processed solar cells for efficient solar energy conversion. The proposed solar cell structure and light trapping scheme are both easily up-scalable with roll-to-roll process, which are highly promising for future industrial productions.

Following the elimination of electrical shorts in the fully-solution-processed solar cells and modification of the bottom PEDOT:PSS electrode with a conjugated polymer interlayer, the active layer performed at an IQE as high as 85%: which is the highest efficiency reported for this type of solar cells. Meanwhile, by using the paper based light trapping element, we achieved a new record efficiency for the fully-solution-processed solar cells.

The trade-off between electrical and optical losses, and their effects on the photovoltaic performance of PEDOT-PEDOT solar cells were theoretically and experimentally investigated: we found that the bottom PEDOT:PSS electrode had to be sufficiently thick to avoid electrical losses, and yet sufficiently thin to transmit light for back-reflection and photon reutilization. Too thick PEDOT:PSS also induced electrical shorts in the device, which led to a high shunt current that limited the FF of the solar cell. Nevertheless, even fully optimized and non-shorted PEDOT-PEDOT solar cells were inherently limited by absorption losses in the electrodes, which limited the absorption gain upon using a back-reflector. Therefore, we believe that future improvements in the photovoltaic performance of PEDOT-PEDOT solar cells rely on the development of high-conductivity and high-transmittance PEDOT:PSS.

Experimental

Materials: High conductivity PEDOT:PSS PH1000 was purchased from H. C. Starck and used as electrode material. PEIE interlayer was purchased from SIGMA-ALDRICH. $PC_{71}BM$ was purchased from Solenne BV. The paper used as a scatterer was provided by StoraEnso. PDMS (base and curing agent 10:1 wt) was deposited via drop-casting on paper, and cured in an oven at a constant temperature of 60 ^{o}C to ensure optical conformal contact with the solar cells. The active donor material TQ1 was synthesized following the method described in reference 23.

Device fabrication: PEDOT-PEDOT solar cells were fabricated on glass substrates cleaned by detergent and followed by TL-1 treatment. Bottom PEDOT:PSS electrode was spin-coated on the clean substrate from an aqueous solution mixed with 5% (vol%) dimethylsulfoxide, 5% (vol%) silquest A-186 silane, and 0.5% (vol) surface Zonyl FS 300, then dried on a hotplate at 60 ^{o}C for 1 min. PEIE interlayer was then spin-coated on top of the PEDOT:PSS at 2000 rpm for 1 min, from an isopropanol diluted solution (0.1%, wt). The active layer was spin-coated on top of the PEIE modified PEDOT:PSS at 500 rpm for 1 min followed by 3000 rpm for 20 s, from a TQ1:$PC_{71}BM$ solution (25 mg ml^{-1}, D:A 2:5, oDCB). The top PEDOT:PSS was then spin-coated at 1000 rpm for 1 min from solution mixed with 5% (vol%) dimethylsulfoxide and 0.5% (vol) surface Zonyl FS 300, and dried on a hotplate at 60 ^{o}C for 1 min. The thickness of the top PEDOT layer is 120 nm, as measured by a Dektak surface profilometer. All PEDOT-PEDOT solar cells studied in this work were encapsulated and had an active area of ≈4 mm2, as calibrated with an optical microscope. The paper reflector was laminated to the backside of the solar cell with the help of the PDMS layer. Therefore, it was electrically separated from the solar cell and it did not induce electric defects.

Device characterization: JV curves were measured by a Keithley 2400 source meter under simulated AM 1.5 illumination with intensity of 100 mW cm^{-2} coming from a SS 50A Photo emission Tech. Light intensity was carefully calibrated by a reference silicon solar cell (SRC-1000-RTD) with a spectral response similar to that of the PEDOT-PEDOT solar cells. A Perkin Elmer Lambda 900 UV-Vis-NIR absorption spectrometer was used for transmittance, reflectance and absorbance measurements. EQE was measured by the Oriel Merlin digital lock-in radiometry under illumination by monochromatic light at short-circuit condition. Photocurrent images were rendered using the LBIC technique, where a pulsed laser (632 nm) is scanned over the active area of the device. The laser spot size was ~100 µm. Photocurrent was collected by a lock-in amplifier from Intermodulation Products AB, after pre amplification in a SR570 pre-amplifier from Stanford Research Systems.

UPS measurements were performed in an ultrahigh vacuum surface analysis system with a SCIENTA-200 hemispherical analyzer and calibrated by determining the Fermi level edge of the Ar^{+} ion sputtered-cleaned Au foil. The HeI resonance line at 21.22 eV was used as the excitation source with a binding energy resolution of 0.05 eV. The work function was derived from the secondary electron cut-off.

Materials extinction coefficients (*k*) and refractive indexes (*n*) were determined by variable angle spectroscopic ellipsometry using a RC2 instrument from J. A. Woollam Co., Inc. Thin films were spin-coated on silicon with a ~1.5 nm native oxide. For modelling of the optical constants CompleteEase, J.A. Woollam Co., Inc. was used. Thus obtained optical constants were further used for transfer matrix modelling.

Paper SEM image was taken with a Leica EM SCD500. Prior to measurements paper was coated with 15 Å Pt. The SEM Leo (Zeiss) was run at > 5kV acceleration voltage using an inlense detector.

Acknowledgements

This work has been supported by the Swedish Energy Agency and the Knut and Alice Wallenberg Foundation through a Wallenberg Scholar grant to O.I, and through the project Power Papers. We thanks Stora Enso for kind supply of paper samples.

Notes and references

1 Y. Liu, J. Zhao, Z. Li, C. Mu, W. Ma, H. Hu, K. Jiang, H. Lin, H. Ade and H. Yan, *Nat. Commun.*, 2014, **5**, 5293.
2 Z. He, B. Xiao, F. Liu, H. Wu, Y. Yang, S. Xiao, C. Wang, T. P. Russell and Y. Cao, *Nat. Photonics*, 2015, **9**, 174-179.
3 J. You, L. Dou, K. Yoshimura, T. Kato, K. Ohya, T. Moriarty, K. Emery, C.-C. Chen, J. Gao, G. Li and Y. Yang, *Nat. Commun.*, 2013, **4**, 1446.
4 B. Azzopardi, C. J. M. Emmott, A. Urbina, F. C. Krebs, J. Mutale and J. Nelson, *Energy Environ. Sci.*, 2011, **4**, 3741–3753.
5 N. Espinosa, M. Hösel, D. Angmo and F. C. Krebs, *Energy Environ. Sci.*, 2012, **5**, 5117–5132.
6 R. G. Brandt, W. Yue, T. R. Andersen, T. T. Larsen-Olsen, M. Hinge, E. Bundgaard, F. C. Krebs and D. Yu, *J. Mater. Chem. C*, 2015, **3**, 1633–1639.
7 Y. Zhou, C. Fuentes-Hernandez, J. Shim, J. Meyer, A. J. Giordano, H. Li, P. Winget, T. Papadopoulos, H. Cheun, J. Kim, M. Fenoll, A. Dindar, W. Haske, E. Najafabadi, T. M. Khan, H. Sojoudi, S. Barlow, S. Graham, J.-L. Brédas, S. R. Marder, A. Kahn and B. Kippelen, *Science*, 2012, **336**, 327–332.
8 Y. Zhou, H. Cheun, S. Choi, W. J. P. Jr, C. Fuentes-Hernandez and B. Kippelen, *Appl. Phys. Lett.*, 2010, **97**, 153304.
9 Y. Zhou, T. M. Khan, J. W. Shim, A. Dindar, C. Fuentes-Hernandez and B. Kippelen, *J. Mater. Chem. A*, 2014, **2**, 3492–3497.
10 F. Guo, T. Ameri, K. Forberich and C. J. Brabec, *Polym. Int.*, 2013, **62**, 1408–1412.
11 W. Yu, L. Shen, P. Shen, Y. Long, H. Sun, W. Chen and S. Ruan, *ACS Appl. Mater. Interfaces*, 2014, **6**, 599–605.
12 K. Tvingstedt, Z. Tang and O. Inganäs, Appl. *Phys. Lett.*, 2012, **101**, 163902.
13 Z. Tang, A. Elfwing, J. Bergqvist, W. Tress and O. Inganäs, *Adv. Energy Mater.*, 2013, **3**, 1606–1613.
14 D. Ha, Z. Fang, L. Hu and J. N. Munday, *Adv. Energy Mater.*, 2014, **4**, 1301804.
15 Z. Fang, H. Zhu, Y. Yuan, D. Ha, S. Zhu, C. Preston, Q. Chen, Y. Li, X. Han, S. Lee, G. Chen, T. Li, J. Munday, J. Huang and L. Hu, *Nano Lett.*, 2014, **14**, 765–773.
16 L. Leonat, M. S. White, E. D. Głowacki, M. C. Scharber, T. Zillger, J. Rühling, A. Hübler and N. S. Sariciftci, *J. Phys. Chem. C*, 2014, **118**, 16813–16817.
17 Z. Tang, W. Tress, Q. Bao, M. J. Jafari, J. Bergqvist, T. Ederth, M. R. Andersson and O. Inganäs, *Adv. Energy Mater*., 2014, **4**, 1400643.
18 J. J. van Franeker, W. P. Voorthuijzen, H. Gorter, K. H. Hendriks, R. A. J. Janssen, A. Hadipour, R. Andriessen and Y. Galagan, *Sol. Energy Mater. Sol. Cells*, 2013, **117**, 267–272.
19 W. Gaynor, J.-Y. Lee and P. Peumans, *ACS Nano*, 2010, **4**, 30–34.
20 F. Guo, X. Zhu, K. Forberich, J. Krantz, T. Stubhan, M. Salinas, M. Halik, S. Spallek, B. Butz, E. Spiecker, T. Ameri, N. Li, P. Kubis, D. M. Guldi, G. J. Matt and C. J. Brabec, *Adv. Energy Mater.*, 2013, **3**, 1062–1067.
21 J. H. Yim, S. Joe, C. Pang, K. M. Lee, H. Jeong, J.-Y. Park, Y. H. Ahn, J. C. de Mello and S. Lee, *ACS Nano*, 2014, **8**, 2857–2863.
22 J. Y. Kim, J. H. Jung, D. E. Lee and J. Joo, *Synth. Met.*, 2002, **126**, 311–316.
23 E. Wang, L. Hou, Z. Wang, S. Hellström, F. Zhang, O. Inganäs and M. R. Andersson, *Adv. Mater.*, 2010, **22**, 5240–5244.
24 O. P. Dimitriev, D. A. Grinko, Y. V. Noskov, N. A. Ogurtsov and A. A. Pud, *Synth. Met*., 2009, **159**, 2237–2239.
25 D. Li and L. J. Guo, *Appl. Phys. Lett*., 2006, **88**, 063513.
26 O. Engström and A. Carlsson, *J. Appl. Phys.*, 1983, **54**, 5245–5251.
27 Z. Tang, L. M. Andersson, Z. George, K. Vandewal, K. Tvingstedt, P. Heriksson, R. Kroon, M. R. Andersson and O. Inganäs, *Adv. Mater.*, 2012, **24**, 554–558.
28 L. A. A. Pettersson, L. S. Roman and O. Inganäs, *J. Appl. Phys.*, 1999, **86**, 487–496.
29 G. F. Burkhard, E. T. Hoke and M. D. McGehee, *Adv. Mater.*, 2010, **22**, 3293–3297.

We report an efficient paper based light trapping element for fully-solution-processed semi-transparent photovoltaic devices with PEDOT:PSS as both electrodes.